IBRACON Structures and Materials Journal
Revista IBRACON de Estruturas e Materiais

ORIGINAL ARTICLE

Assessment of stiffness and structural behavior of reinforced concrete beams rehabilitated with CFRP and crack injection

Avaliação da rigidez e do comportamento estrutural de vigas de concreto armado reabilitadas com CFRP e injeção de fissuras

Luis Felipe Fernandes Guim[a] iD
Gustavo Emilio Soares de Lima[a] iD
Gustavo de Souza Veríssimo[a] iD
José Luiz Rangel Paes[a] iD

[a]Universidade Federal de Viçosa – UFV, Departamento de Engenharia Civil, Viçosa, MG, Brasil

Abstract: In this paper, an experimental program was developed in order to evaluate the structural behavior of RC beams rehabilitated with CFRP sheets and crack injections. The specimens' stiffness before and after structural rehabilitation was assessed through vibration tests. Bending tests were employed to obtain load-deflection curves and evaluate failure modes. Results indicate that all beams displayed higher stiffness values after structural rehabilitation. The CFRP sheet fostered an increase of the specimens' ultimate load. Crack injections influenced stiffness but did not affect the ultimate load.

Keywords: structural rehabilitation; NDT; RC beam; reinforcements with CFRP; crack injection.

Resumo: Neste trabalho, foi desenvolvido um programa experimental com o objetivo de avaliar o comportamento estrutural de vigas de concreto armado reabilitadas com manta de CFRP e injeções de fissuras. A rigidez dos modelos antes e depois da reabilitação estrutural foi avaliada por meio de ensaios de vibração. Foram realizados ensaios de flexão para obter curvas de carga-flecha e avaliar modos de falha. Os resultados indicam que todas as vigas apresentaram valores de rigidez mais elevados após a reabilitação estrutural. A manta de CFRP promoveu um aumento da carga final dos modelos. As injeções de fissura influenciaram a rigidez, mas não afetaram a carga final.

Palavras-chave: reabilitação estrutural; END; viga de concreto armado; reforço com CFRP; injeção de fissuras.

1 INTRODUCTION

According to the fib Model Code for Concrete Structures [1], a structure is considered durable when it meets performance requirements throughout the lifespan specified in its project. In cases where these requirements are not met, structural rehabilitation procedures must be conducted if the structure is to remain operational. According to Souza and Ripper [2], these procedures can be used to meet service and durability conditions (repair) or to increase or reestablish the structure's bearing capacity (reinforcement), which requires additional materials.

In the case of reinforced concrete members subject to bending, the cracking process, albeit inevitable, may influence the structure's performance. von Fay [3] states that excessive cracking can expose the reinforcement bars to the action of external agents and reduce the element's stiffness. According to this author, cracks with openings between 0.05mm

and 6.3mm should be injected with epoxy resins for structural repair purposes. These resins react with the concrete, producing very resistant solids with a relatively high modulus of elasticity. Al-Nu'man and Al-Sahlani [4] present studies from several authors who affirm that a structure restored with crack injection can show an ultimate resistance and stiffness equivalent to that of the earlier undamaged monolithic structure.

In order to increase or reestablish the ultimate resistance of a structure subject to bending, Beber [5] cites that reinforcing with CFRP is a good option, especially due to their mechanical properties. CFRP presents a large resistance/self-weight ratio, performing well at high temperatures. Juvandes and Figueiras [6] highlight that the fibers possess linear elastic behavior and brittle failure, with ultimate strength at 3500 MPa, modulus of elasticity varying between 150 GPa and 600 GPa, and maximum elongation at approximately 1.5%. CFRP reinforcement work like tensioned steel for reinforced concrete elements. The analysis and design of elements reinforced with CFRP subject to bending can be done using the same regular hypotheses applied to reinforced concrete elements, with an additional verification limiting the fiber's strain to avoid debonding [7], [8]. According to Salgado et al. [9] although CFRP reinforcements improve an element's ultimate resistance, they exert little influence over its stiffness.

In order to know the residual characteristics of structural elements, which are necessary for decision-making in the structural rehabilitation process, non-destructive testing (NDT) is often conducted, as pointed by Helal et al. [10]. Salawu [11] presents studies demonstrating that vibration analysis has been widely employed to obtain information about the mechanical characteristics of structures. The modal parameters of a given structure (natural frequencies, mode shapes, and modal damping) are sensitive to alterations in the structure's physical parameters (mass and stiffness). Any alteration in a structural element's stiffness is directly related to a change in its natural vibration frequencies, depending also on boundary conditions and support stiffness. With the aid of vibration analyses and conventional bending tests, the increase in stiffness and ultimate resistance of reinforced concrete beams rehabilitated with CFRP and crack injection can be assessed.

The purpose of this paper is to evaluate the stiffness of beams rehabilitated with CFRP, with and without crack injection, in order to provide a more realistic evaluation of their structural behavior. Currently there are no recommendations regarding which stiffness percentage is acceptable in the evaluation of the behavior of rehabilitated structural elements. Moreover, most of the research on beams reinforced with CFRP employed test specimens that were perfectly whole. The rehabilitation of damaged elements adopted in this work resembles real situations of structural rehabilitation more closely. This can contribute to a better understanding of the behavior of reinforced structures.

2 MATERIALS AND EXPERIMENTAL PROGRAM

2.1 Specimens

This study employed nine specimens that were initially produced in the context of Lima's [12] research. The dimensions of all beams were 9 x 18 x 180 cm. The beams' concrete had a water/cement ratio of 0.60 and three different steel reinforcement ratios, resulting in three different groups of three specimens with the same reinforcement ratio in each group. Figure 1 displays general schematics of the beams.
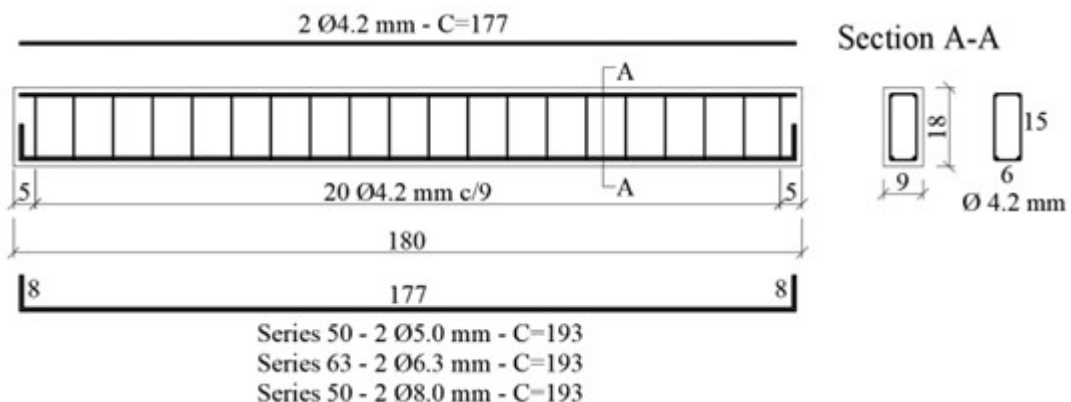

Figure 1. Schematics of original undamaged specimens. Dimensions in centimeters unless otherwise specified.

The original models were subjected to bending tests, with a vertically induced load from top to bottom, causing tensile stress on the element's lower surface. In these tests all models failed due to steel yielding. The tests also caused permanent deflection in all models. The models were displayed with the surface that suffered tension turned upwards to facilitate the observation of deflections and cracks as shown in Figure 2. The beams' state of degradation after the bending test performed by Lima [12] – before rehabilitation procedures – can also be seen in this figure.

(a)   **(b)**
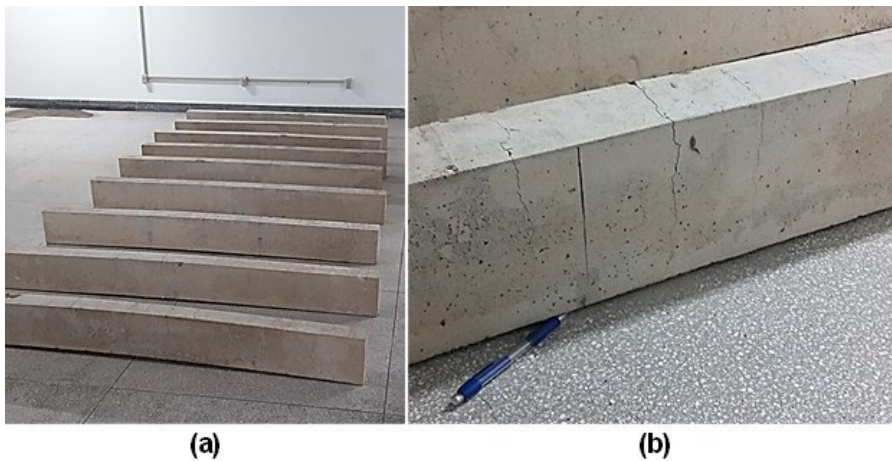
Figure 2. Original specimens after mechanical d'+amage (a); detail of cracking and permanent deflection (b).

A preliminary inspection of the damaged beams was conducted in order to select which materials and procedures should be adopted for the rehabilitation. Table 1 contains a summary of the general characteristics of the beams used in this work. Codes 50, 63, and 80 represent beams with positive reinforcements of $2\phi5.0$, $2\phi6.3$, and $2\phi8.0$, respectively. Codes R1, R2, and R3 represent specimen numbers.

Table 1. Specimen characteristics.

	Series	50			63			80		
	Specimen	**R1**	**R2**	**R3**	**R1**	**R2**	**R3**	**R1**	**R2**	**R3**
Technical features	E_s (MPa)		210000			210000			210000	
	f_c (MPa)		50.2			50.2			50.2	
	$f_{ct,m}$ (MPa)		3.6			3.6			3.6	
	E_c (MPa)		26880			26880			26880	
	Ultimate load (kN)	19.61	19.43	19.82	26.64	26.40	25.66	43.96	47.75	48.06
	EI x 10^5 (Nm^2) - Initial	9.71	10.52	10.87	9.84	9.61	9.89	9.80	9.91	10.34
	EI x 10^5 (Nm^2) - Final	4.12	3.80	4.37	5.62	5.43	5.60	5.66	4.95	5.20
	Biggest crack (mm)	0.70	0.83	0.77	0.90	0.60	0.70	0.63	0.70	0.53
	Smallest crack (mm)	0.23	0.20	0.20	0.20	0.40	0.30	0.30	0.40	0.13
	Permanent deflection (mm)	4.81	4.62	4.62	4.35	4.61	4.67	7.11	11.17	8.10

The three beam specimens of each group, which had the same reinforcement ratio, underwent different structural rehabilitation procedures. The first specimen did not undergo crack injection. The cracks on the second specimen were injected with resin type 1, recommended for cracks larger than 0.3 mm. The cracks on the third specimen were injected with resin type 2, recommended for cracks larger than 0.1 mm. After the injection procedure, all specimens were reinforced with a CFRP sheet. Table 2 shows the nomenclature used to identify each specimen in relation to its characteristics. The prefix CR represents the reinforcement with the carbon fiber sheet (CFRP sheet). The number next to the prefix represents the diameter of the rebars. The suffix indicates which injection process was adopted: NI (no injection), I1 (injection with resin type 1), and I2 (injection with resin type 2).

Table 2. Specimen IDs according to structural rehabilitation process.

Reinforcement	Rehabilitation Process			ID
		Injection		
Ц (mm)	Carbon Reinforcement	Resin type 1 (> 0.3 mm)	Resin type 2 (> 0.1 mm)	
5.0	x			CR50-NI
5.0	x	x		CR50-I1
5.0	x		x	CR50-I2
6.3	x			CR63-NI
6.3	x	x		CR63-I1
6.3	x		x	CR63-I2
8.0	x			CR80-NI
8.0	x	x		CR80-I1
8.0	x		x	CR80-I2

CR-## – CR50 - 2ϕ5.0, CR63 - 2ϕ6.3; CR80 - 2ϕ8.0.
NI – No injection; I1 – Injection with resin type 1; I2 – Injection with resin type 2.

2.2 Crack injections

Table 3 displays the physical and mechanical characteristics of the two different resins used in the crack injections.

Table 3. Characteristics of resins

Epoxy resin	Penetration	c (g/cm³)	Visc. (mPa·s)	$\gamma_{comp.}$ (MPa)	$\gamma_{trac.}$ (MPa)	e_{max}	E (MPa)
Type 1	≥ 0.3 mm	1.08	300	70	30	6.0%	2600
Type 2	≥ 0.1 mm	1.07	145	75	65	4.5%	3000

Due to the models' small size, surface packers were utilized in the injection process (Figure 3), same procedure utilized by Ekenel and Myers [13], Nikopour and Nehdi [14] and Griffin et al. [15]. The alternative would be to employ borehole packers, which is an invasive procedure that could cause damage to the models and undermine the final rehabilitation process.
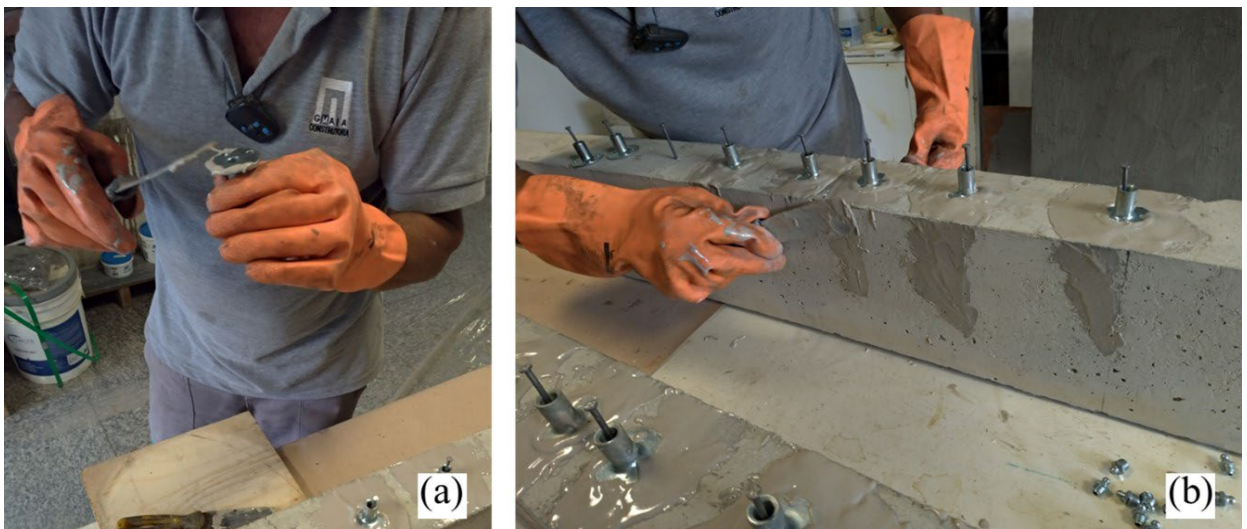

Figure 3. Surface packers.

For one single crack, epoxy resin manufacturers usually recommend a distance between surface packers smaller than the structural element's thickness. In the models employed in this study, the cracks spanned the entire width of the transversal section, which was small. For this reason, only one surface packer was placed over each crack, contributing to the resin's penetration. The packers were secured with a nail after being glued to the specimen. The placement of the surface packers is displayed in Figure 4.

Figure 4. Surface packers secured with nails.

After the beams were cleaned, the cracks were sealed and the surface packers were glued with an epoxy adhesive and secured with nails. In Figure 5 one can observe the gluing of the surface packers and the superficial sealing of each crack, which extended through the entire lateral section. All cracks visible to the naked eye on the surface of the model that underwent tension were injected.

Figure 5. Gluing of surface packers (a); sealing the cracks (b).

The cracks received epoxy resin injections after the sealing adhesive finished curing. The bicomponent resin was mixed and all cracks were injected as shown in Figure 6.
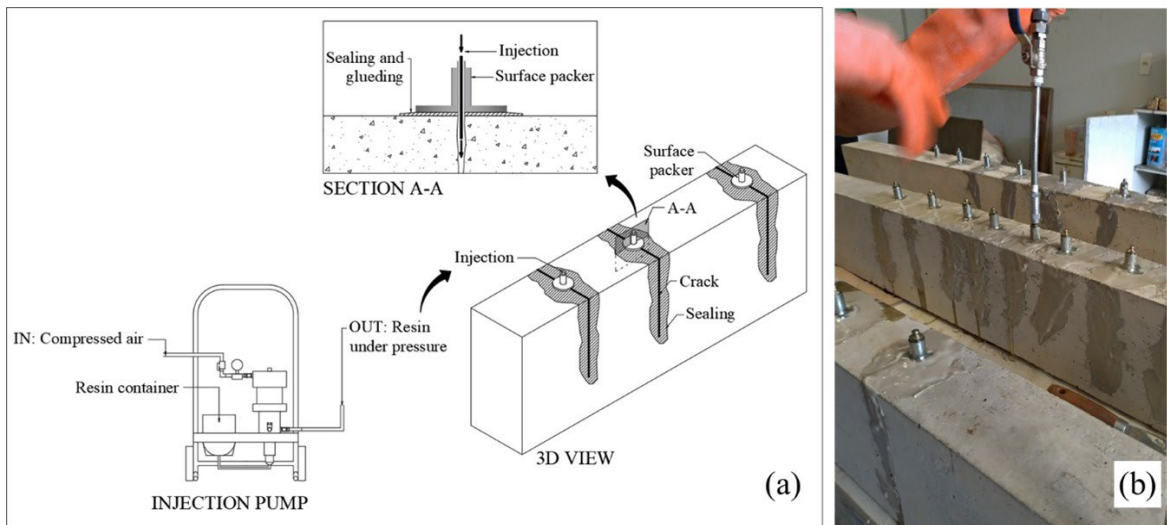
Figure 6. General schematics of crack injection in the models (a); crack injection procedure (b)

The entire injection process was performed with pressures varying between 35 bar and 100 bar, values below the 200 bar recommended by the manufacturer as the maximum pressure for crack injection. The injection procedure of each crack was finished when the injected material overflowed.

2.3 Reinforcement with CFRP sheet

The structural reinforcement with the CFRP sheet was done after the beams' cracks were injected. All surface packers were removed before the structural reinforcement with CFRP was carried out. The adhesive employed in the sealing of cracks and gluing of surface packers was also removed with a grinding machine.

The flexural reinforcement was designed according to the ACI 440.2R [8]. The ultimate load reached in each specimen of Lima's [12] work was adopted as design criteria. All elements were reinforced with a single layer of CFRP. For specimens CR63 and CR80, where ultimate loads surpassed that of specimen CR50, a transverse anchorage was necessary in order to meet criteria established in the ACI 440.2R [8]. Figure 7 displays the schematics of beams reinforced with CFRP. Table 4 indicates the physical and mechanical characteristics of materials employed in the reinforcement.
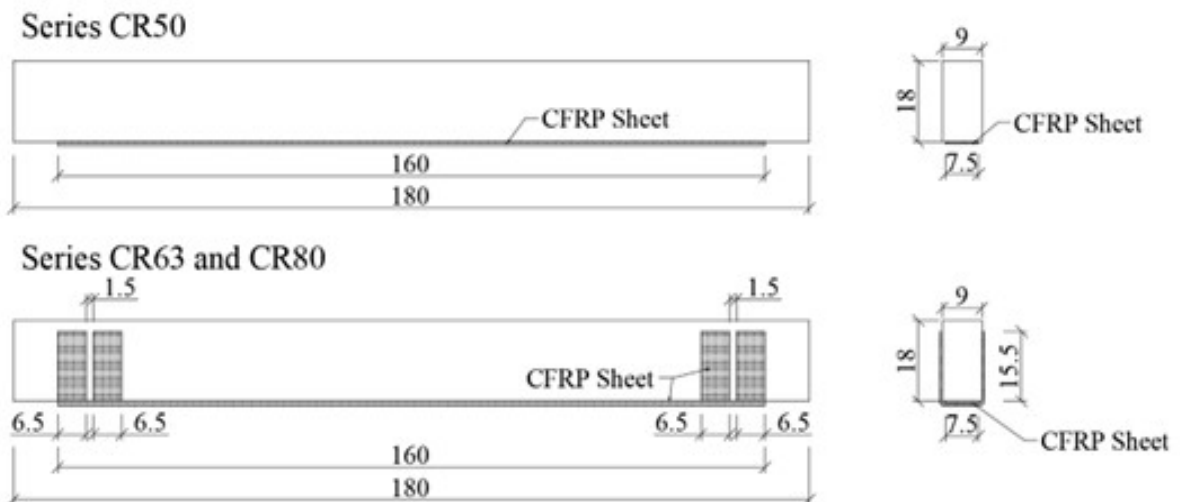

Figure 7. Schematics of beams reinforced with CFRP sheet. Dimensions in centimeters.

Rev. IBRACON Estrut. Mater., vol. 16, no. 1, e16110, 2023

6/16

Table 4. Characteristics of materials employed in reinforcements with CFRP

	c	$y_{trac.}$	$y_{ader.}$	E	e_{max}	t
	(g/m^2)	(MPa)	(MPa)	(MPa)	(%)	(mm)
CFRP sheet	300	3600	-	230000	2.1	0.166
Thixotropic adhesive	1.33	-	14	4700	-	-
Laminating resin	1.12	-	14	3000	-	-

The regions where CFRP sheets were attached (lower part and the sides that received anchorage) were sanded with a grinder in order to expand the concrete's pores and contribute to its bonding to the thixotropic adhesive. Subsequently, the concrete's surface was cleaned in order to remove dust particles, grease, or any other contaminant that might hinder adherence.

The lamination resin was applied after the thixotropic adhesive finished curing, with the sheet already attached. A foam paint roller was used to drench the CFRP sheet in the lamination resin, ensuring that the carbon fiber sheet was completely soaked with resin. Figure 8 shows part of the beam specimens after the rehabilitation process, highlighting the lower faces where the CFRP sheet was applied.
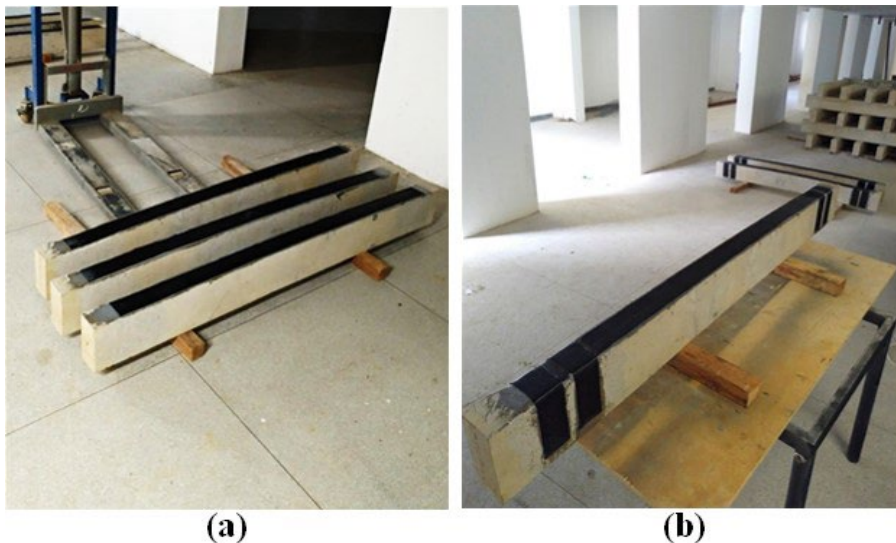
Figure 8. Beams reinforced with CFRP without anchorage (a), and with anchorage (b).
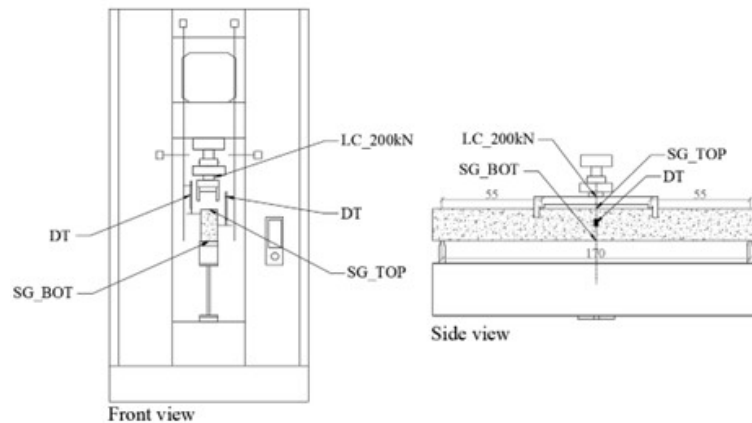
2.4 Bending test

The bending test followed the same procedure employed in the reference experiments conducted by Lima [12]. The Stuttgart Test configuration was adopted, with four load application points. Loads were applied 55 cm away from supports and were 60 cm apart, as shown in Figure 9.
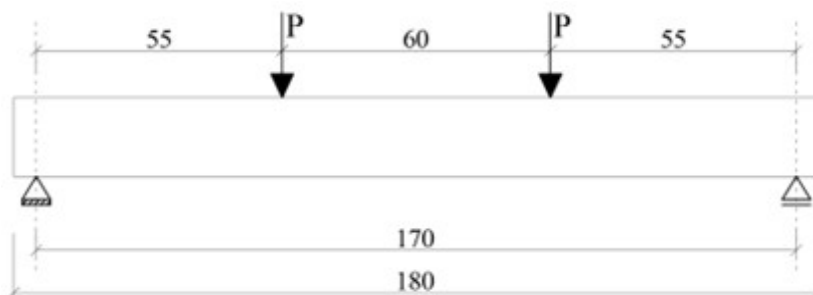
Figure 9. Bending test structural model. Dimensions in centimeters

Rev. IBRACON Estrut. Mater., vol. 16, no. 1, e16110, 2023

7/16

The load was applied continuously with displacement control at a rate of 0.01 mm/s. The steel reaction beam was strategically placed over the universal testing machine in order to provide a 170 cm span for the specimens.

Two displacement transducers (DT) were installed in the center of the span in order to measure displacements. Additionally, two strain gauges were employed, both placed on the piece's central axis. One of the strain gauges was placed on the top of the element (SG_TOP) and the other at the bottom (SG_BOT) to measure deformations in the concrete and in the carbon fiber, respectively. A 200kN load cell was placed between the load transmission device and the actuator's spherical seating in the universal testing machine. Figure 10 displays the bending test's assembly schematics.


Figure 10. Bending test assembly schematics. Dimensions in centimeters.

The beam specimens were subjected to progressive load stages where displacement and deformations were measured. At the end of each stage the load was completely removed, the actuator having been suspended, reestablishing the beam's original simply supported condition. This procedure restores the element's elastic deformation while maintaining the inelastic deformation resulting from each stage.

2.5 Vibration test

The beams were instrumented as shown in Figure 11, with an accelerometer in position 1. The beam was struck with a rubber hammer in position 2 so that its fundamental frequency could be obtained.

① Accelerometer placement point
② Impact application point
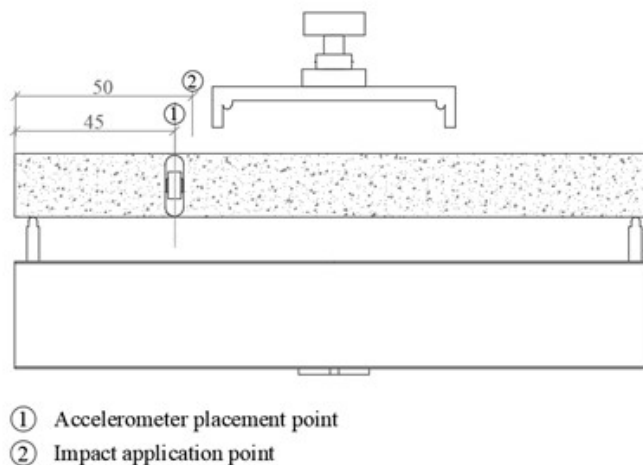
Figure 11. Accelerometer placement and impact application point in the vibration test.

Rev. IBRACON Estrut. Mater., vol. 16, no. 1, e16110, 2023

8/16

The vibration test of specimens was performed before and after rehabilitation procedures. In both cases, the beam was simply supported. The fundamental frequency of each specimen was determined through the Fast Fourier Transform (FFT) applied to acceleration and time data.

After the fundamental vibration frequency was obtained, with the simply supported boundary condition maintained, the stiffness was calculated according to Equation 1 [16].

$$EI = \frac{f^2 (2\pi L^2)^2 (\rho A)}{(\beta^2)^2} \tag{1}$$

where: f = fundamental vibration frequency (Hz); L = span (m); ρ = beam's specific mass (kg/m³); A = cross-section area (m²); β^2 = constant dependent on boundary conditions (9.869).

3 RESULTS AND DISCUSSION

3.1 Stiffness after the rehabilitation process

Based on acceleration and frequency values obtained in the vibration tests, the stiffness before and after structural rehabilitation was estimated through Equation 1. Figure 12 displays the stiffness of each beam specimen before and after rehabilitation, as well as the stiffness values of the original undamaged beams obtained by Lima [12].
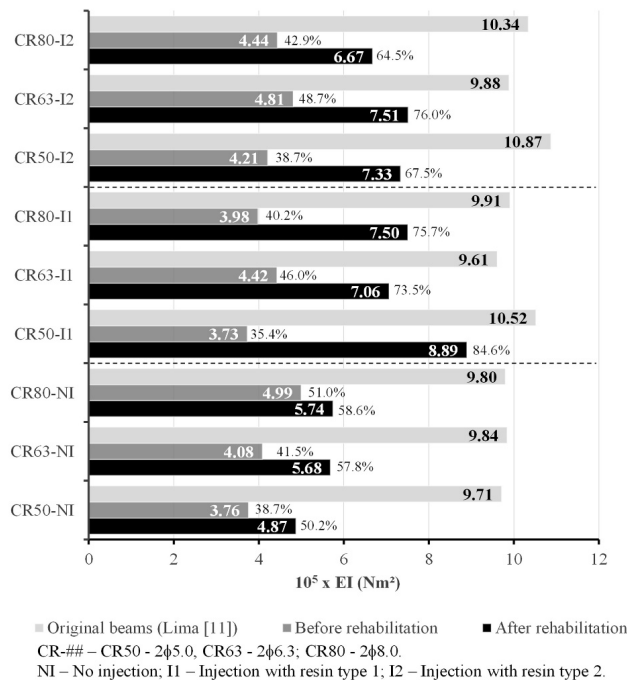
Figure 12. Estimated stiffness of the beams.

After structural rehabilitation, elements that went through the injection process and were reinforced with CFRP (CR##-I1 and CR##-I2) displayed an average stiffness of 74% of the original beams' stiffness, as observed in the results shown in Figure 12. In contrast, elements that were only reinforced with CFRP and were not injected (CR##-NI) displayed an average 55% of the original specimens' stiffness. Therefore, in both cases (with and without crack injection) stiffness was higher than the estimated stiffness of damaged specimens before rehabilitation. It is also evident that specimens with crack injection (CR##-I1 and CR##-I2) displayed a stiffness superior to those only reinforced with

CFRP (CR##-NI). These results confirm what was observed by Salgado et al. [9] and by Al Nu'man and Al-Sahlani [4] regarding the influence of the rehabilitation process in the element's stiffness.

Resin type 2 (less viscous) was expected to re-establish a higher degree of the element's original monolithic configuration since, unlike resin type 1, it would also fill cracks with openings between 0.1 mm and 0.3 mm. However, stiffness results did not corroborate this expectation as seen in Figure 12. Based on the estimated stiffness after injection, beam stiffness results for both resins fell in the same range.

Figure 13 displays load-deflection curves obtained in the bending tests. In addition to test curves, one extra curve has been plotted based on the analytical model proposed by Branson [17], which considers the CFRP sheet in the same way as the reinforcement bars for purposes of cross-section homogenization.
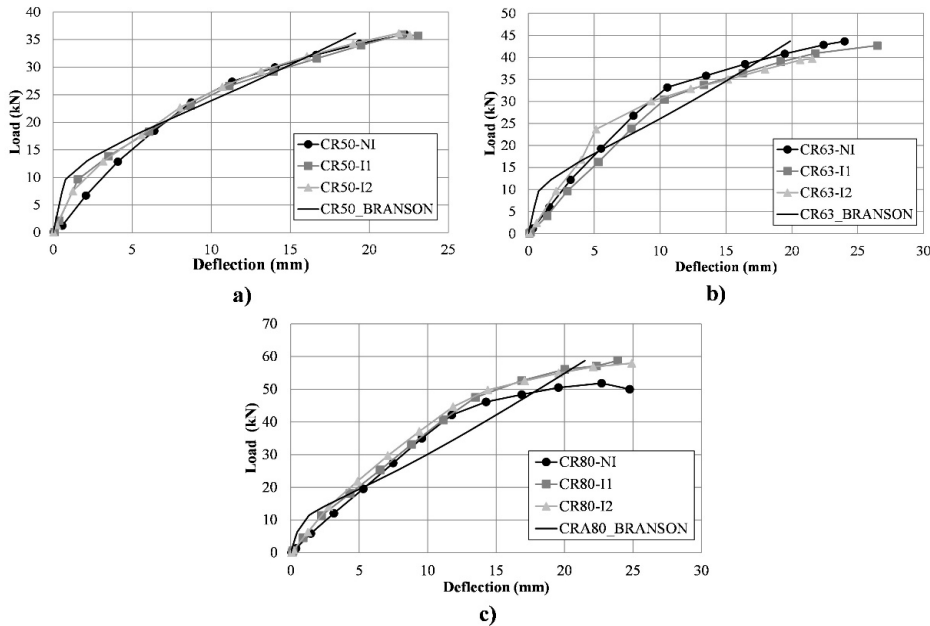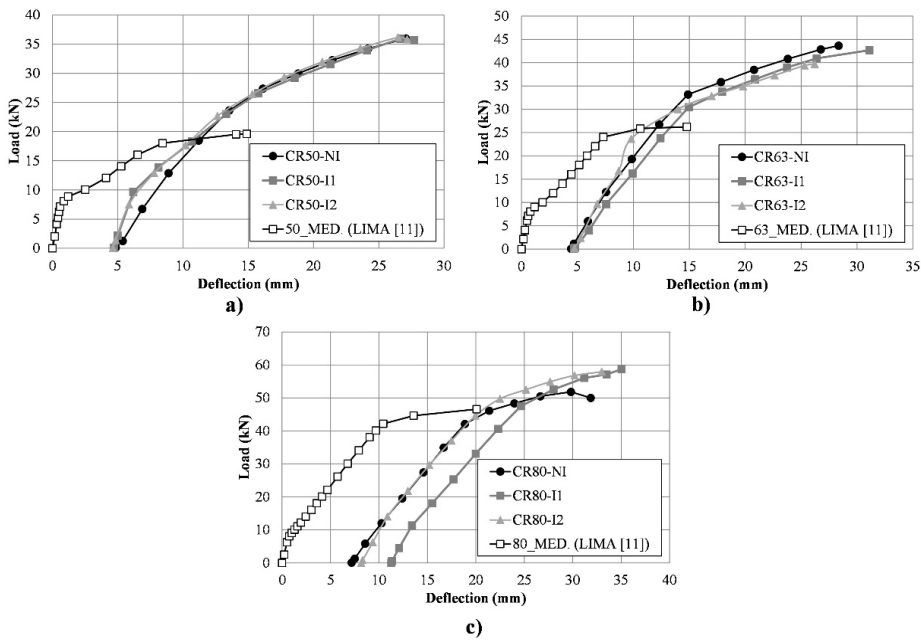

Figure 13. Load-deflection curves obtained in the bending test for beams: a) CR50; b) CR63; c) CR80. Load (kN) represents the sum of the loads (2*P*) applied to the beam.

By observing curve slopes in Figure 13, one can note a difference in element stiffness during initial load stages. This difference is related to the adoption of the structural rehabilitation process. Non-injected beams (CR##-NI) had a lower initial stiffness than injected beams, except for beam CR63-NI. This lower initial stiffness in non-injected specimens is consistent with the results obtained with vibration tests, displayed in Figure 12. Moreover, the difference in stiffness becomes less pronounced during load application and the stiffness decay level tends to be the same in all beams in stages with more elevated loads.

When experimental results and analytically estimated results are compared, it is evident that Branson's analytic model [17] predicts a higher initial stiffness. This model considers that the parts are uncracked at the beginning of the test. However, according to what has been observed in the vibration tests, in the case of rehabilitated elements, not even parts that underwent crack injections with epoxy resins displayed a stiffness level equal to that of uncracked parts. Therefore, the difference in stiffness during initial load stages that can be seen in the load-displacement curves is due to a degradation already present in all elements.

3.2 The structural behavior of rehabilitated beams

Figure 14 displays load-displacement curves obtained through the bending test. The deflection relative to each load stage corresponds to the deflection obtained in the test added to the residual deflection measured prior to testing, according to figures presented in Table 1. The average curve of the original undamaged specimen tests obtained by Lima [12] is also displayed with each group of beams with the same reinforcement ratio. This allows for the comparison of the original specimens' behavior as tested by Lima [12] and after structural rehabilitation.

Figure 14. Load-deflection curves comparing rehabilitated beams with the original undamaged beams tested by Lima [12]: a) CR50; b) CR63; c) CR80. Load (kN) represents the sum of the loads (2P) applied to the beam.

Based on Figure 14, one can note that non-injected elements (CR##-NI) presented a stiffness like that of the original beam in State II (##_MED). In contrast, the stiffness of beams that underwent the crack injection procedure (CR##-I1 and CR##-I2) was lower in comparison to the original beam in State I (##_MED), but higher in State II. After the injected beams' (CR##-I1 and CR##-I2) cracking load was reached, which is evident in the inclination change seen in the load-displacement curve, their stiffness remained close to that of the original beams in State II (##_MED) and to that of the non-injected reinforced beams (CR##-NI).

Figure 15 displays ultimate load values reached in the testing of the original undamaged beams and of the reinforced beams, as well as the ultimate load estimated according to design specifications in the ACI 440.2R [8]. The three specimens in each group, which had the same rebars and received reinforcements, displayed similar ultimate loads, indicating that the injection procedure did not influence the ultimate load level. CFRP sheet reinforcements significantly increased ultimate load, especially in the CR50 beams, which displayed an increase in resistance of 84% in comparison to the original undamaged specimens. Moreover, all ultimate loads in the tests surpassed those predicted by design specifications in the ACI 440.2R [8].

	CR50-NI	CR50-I1	CR50-I2	CR63-NI	CR63-I1	CR63-I2	CR80-NI	CR80-I1	CR80-I2
Original beams	19.61	19.43	19.82	26.64	26.40	25.66	43.96	47.75	48.60
ACI 440.2R-08	26.44	26.34	26.54	32.93	32.81	32.44	46.39	47.56	48.44
Tests	35.97	35.94	36.15	43.66	42.68	39.73	51.84	58.72	57.94
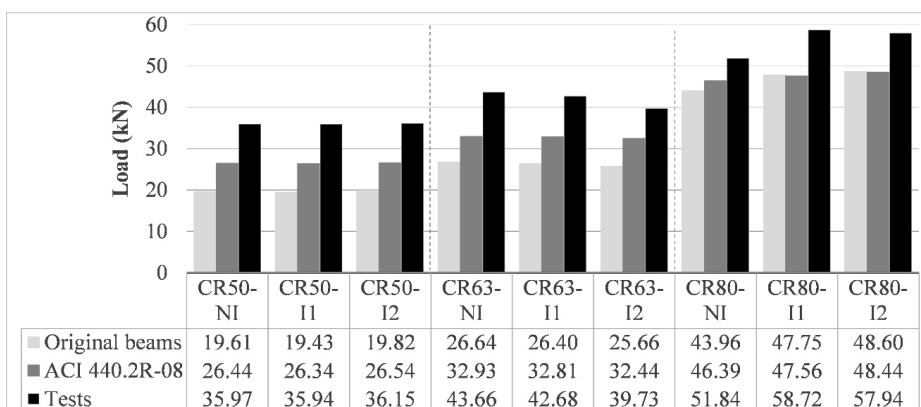
Figure 15. Ultimate loads obtained for the original beams based on design specifications in the ACI 440.2R [8] and through tests. Load (kN) represents the sum of the loads (2P) applied to the beam.

Beams with the same reinforcement ratio displayed similar failure modes. The maximum values reached for load, deflection and deformation can be seen in Figure 16, along with a sketch exemplifying the failure mode of each beam. Note that concrete deflection and deformation results include residual values already present before the test.
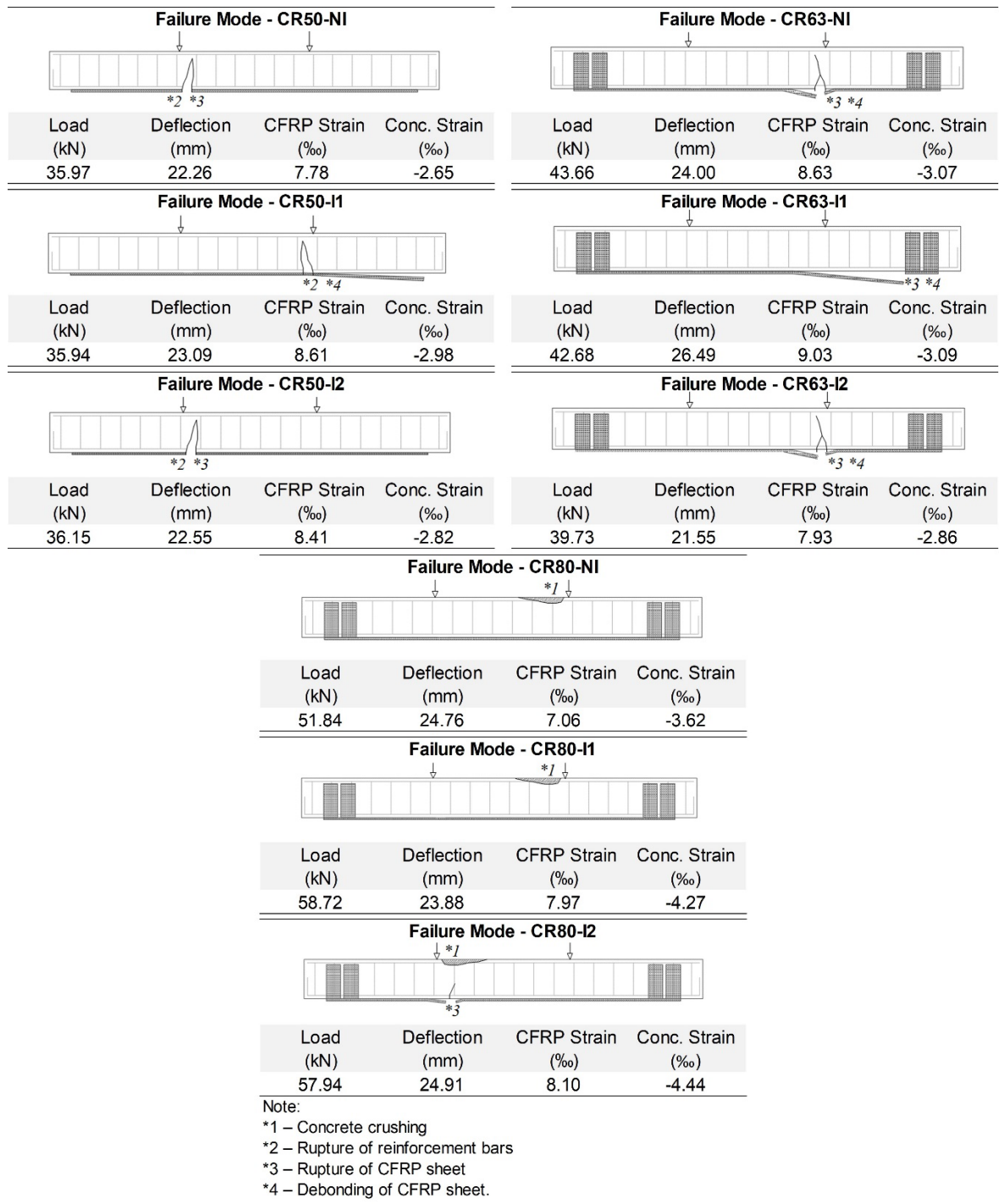

Failure Mode - CR50-NI

Load (kN)	Deflection (mm)	CFRP Strain (‰)	Conc. Strain (‰)
35.97	22.26	7.78	-2.65

Failure Mode - CR63-NI

Load (kN)	Deflection (mm)	CFRP Strain (‰)	Conc. Strain (‰)
43.66	24.00	8.63	-3.07

Failure Mode - CR50-I1

Load (kN)	Deflection (mm)	CFRP Strain (‰)	Conc. Strain (‰)
35.94	23.09	8.61	-2.98

Failure Mode - CR63-I1

Load (kN)	Deflection (mm)	CFRP Strain (‰)	Conc. Strain (‰)
42.68	26.49	9.03	-3.09

Failure Mode - CR50-I2

Load (kN)	Deflection (mm)	CFRP Strain (‰)	Conc. Strain (‰)
36.15	22.55	8.41	-2.82

Failure Mode - CR63-I2

Load (kN)	Deflection (mm)	CFRP Strain (‰)	Conc. Strain (‰)
39.73	21.55	7.93	-2.86

Failure Mode - CR80-NI

Load (kN)	Deflection (mm)	CFRP Strain (‰)	Conc. Strain (‰)
51.84	24.76	7.06	-3.62

Failure Mode - CR80-I1

Load (kN)	Deflection (mm)	CFRP Strain (‰)	Conc. Strain (‰)
58.72	23.88	7.97	-4.27

Failure Mode - CR80-I2

Load (kN)	Deflection (mm)	CFRP Strain (‰)	Conc. Strain (‰)
57.94	24.91	8.10	-4.44

Note:
*1 – Concrete crushing
*2 – Rupture of reinforcement bars
*3 – Rupture of CFRP sheet
*4 – Debonding of CFRP sheet.

Figure 16. Failure modes displayed by the specimens. Load (kN) represents the sum of the loads (2P) applied to the beams.

All CR50 beams displayed reinforcement bar failure associated to the rupture or debonding of the CFRP reinforcement. This indicates that the reinforcement bars ruptured first, causing the entire traction load to fall upon the CFRP reinforcement, causing its failure (Figure 17).
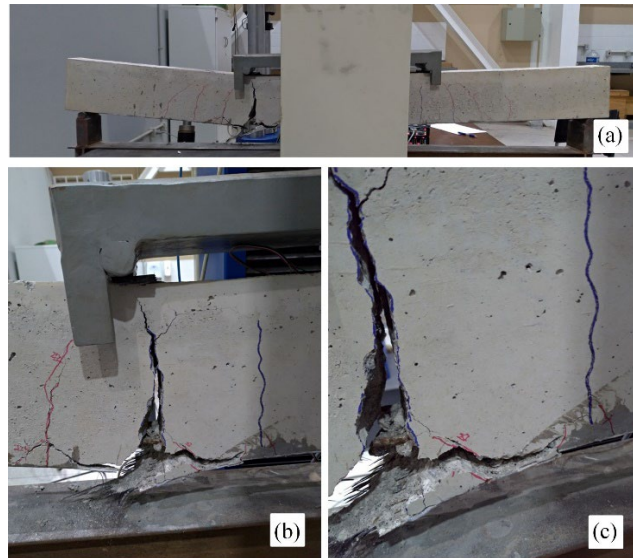

Figure 17. Failure of specimen CR50-NI (a); Detail of the specimen's failure location (b);
Detail of the rupture of the CFRP sheet and positive reinforcement (c).

CR63 beams displayed failure due to the rupture of the CFRP sheet combined with its debonding from the concrete surface. A horizontal failure surface and a high cracking level were evident, characterizing failure due to the reinforcement's sudden peel off caused by shear cracks. The detachment of concrete parts previously joined to the reinforcement was also observed (Figure 18).


Figure 18. Failure of beam CR63-NI (a); Detail of the rupture and debonding of the CFRP sheet (b); Detail of the non-rupture of the positive reinforcement (c).

All beams in the CR80 series displayed the same failure mode, which was the crushing of the compressed concrete. Figure 19 displays the failure mode seen in specimen CR80-I2. In all cases, the concrete's deformation was greater than 3.5‰, corroborating its behavior. Moreover, CR80 beams showed a 20% difference in ultimate load in comparison to the ultimate load predicted by the ACI 440.2R [8], while for the other beams this difference was approximately 30%. This may be related to the failure mode, which occurred in the tensioned region in CR50 and CR63 elements and in the compressed region of CR80 elements.
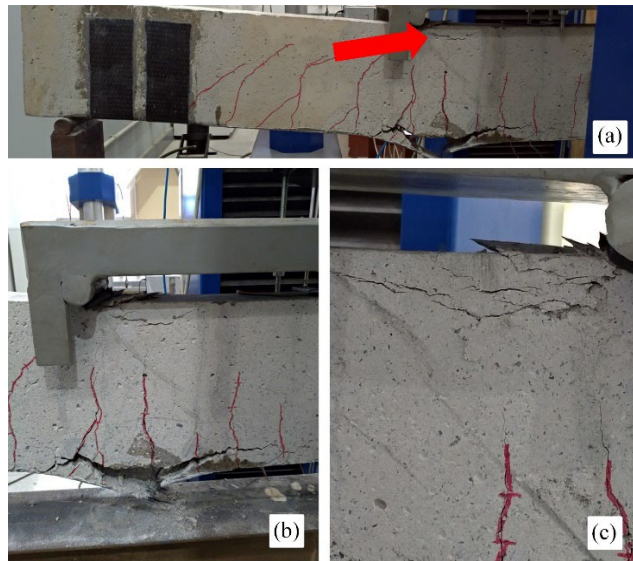
Figure 19. Failure of beam CR80-I2 (a); Detail of the crushed concrete and of the CFRP sheet rupture (b); Magnified detail of the crushed concrete (c).

Non-injected beams suffered an increase in already-present cracks and the emergence of new cracks throughout the element. Specimens that received epoxy resin injections reached failure with a cracking pattern similar to that of non-injected specimens, but only displayed cracks that spawned during testing. Injected cracks did not reopen and new cracks appeared in the surroundings of those that had been injected, as shown in Figure 20. In some cases, the new cracks crossed previously injected cracks, confirming the efficacy of the injection process and the successful recovery of monolithism in the previously cracked region.
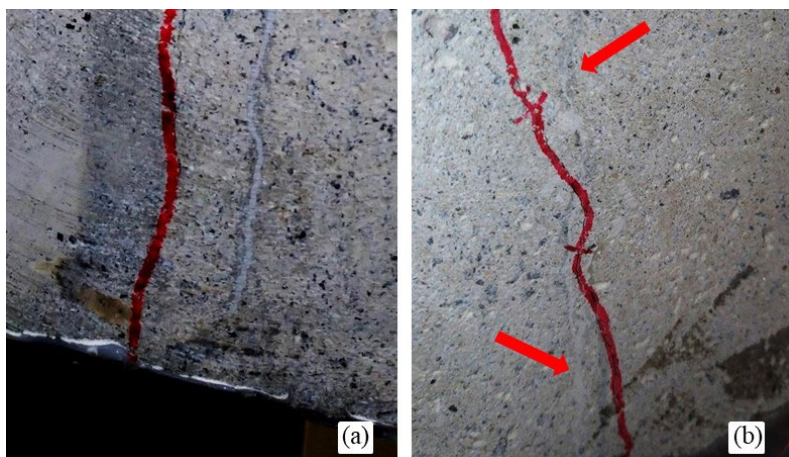
Figure 20. Detail of a new crack next to an injected crack (a); Detail of a new crack crossing an injected crack (b).

5 CONCLUSIONS

This work employed vibration tests, a non-destructive test (NDT), in order to evaluate the structural behavior of reinforced concrete beams rehabilitated with CFRP and crack injection. The main conclusions reached in this study are presented below:

(1) All specimens displayed an increase in their fundamental vibration frequency and, consequently, in their stiffness after the structural rehabilitation process. The crack injections with epoxy resins were responsible for this increase in stiffness. Beams that received crack injections (CR##-I1 and CR##-I2) displayed an average stiffness of 74% of the original undamaged beams' (##_MED) stiffness, while non-injected beams (CR##-NI) displayed around 55% of the original beams' stiffness. Additionally, there were no significant changes regarding the stiffness increase in beams injected with the resin indicated for cracks larger than 0.3 mm (type I1) and in those injected with the resin indicated for cracks larger than 0.1 mm (type I2).

(2) The curve based on the analytical model proposed by Branson [17] displays an initial segment with more inclination than the one obtained experimentally, since this model considers that parts are perfectly monolithic at the beginning of the test. It was evident, however, that even parts subjected to crack injections do not display the same stiffness of the original parts.

(3) Rehabilitated beams displayed an increase in their ultimate load when compared to the original specimens. It is noted that the crack injection process did not influence the ultimate load reached by beams in the bending test. However, non-injected beams (CR##-NI) display a stiffness very similar to the original beams' State II (##_MED). In contrast, the initial stiffness of injected beams (CR##-I1 and CR##-I2), remained between that of the original beams' (##_MED) State I and State II. After reaching cracking load, the injected beams' (CR##-I1 and CR##-I2) stiffness was very close to that of the original beams' State II (##_MED) and to that of the non-injected beam (CR##-NI).

(4) The failure modes of beams with the same reinforcement ratio were similar. All CR50 beams displayed reinforcement bar failure along with the rupture or debonding of the CFRP sheet. CR63 beams displayed failure due to the CFRP's rupture combined with its debonding from the concrete surface. In these cases, a detachment of concrete parts that were previously joined to the rebars also occurred. All CR80 beams displayed failure due to the compressed concrete's crushing. It is noted that in all cases the ultimate load value was superior to the value predicted by the ACI 440.2R [8].

REFERENCES

[1] Federation Internacional du Betón. *fib Model Code for Concrete Structures 2010*, Wiley-VCH Verlag GmbH & Co. KGaA, Weinheim, Germany, 2013. https://doi.org/10.1002/9783433604090.

[2] V. C. Souza and T. Ripper, *Pathology, recovery and structural reinforcement of concrete*, 1st ed. São Paulo, Brazil: Pini, 1998.

[3] K. F. von Fay, *Guide to Concrete Repair*, 2th ed., US Department of the Interior Building – Bureau of Reclamation, Washington, DC, 2015.

[4] B. S. Al-Nu'man and M. H. Al-Sahlani, "Behavior of repaired reinforced concrete beams failed in shear," *J Eng Dev*, vol. 10, no. 3, pp. 115–134, Sep 2006.

[5] A. J. Beber, "Structural behavior of reinforced concrete beams reinforced with carbon fiber composites", Ph.D. dissertation, Univ. Fed. do Rio Grande do Sul, Porto Alegre, Brasil, 2003.

[6] L.P. Juvandes and J.A. Figueiras, "Design and security concepts for reinforcement projects with composite FRP systems", *Concr. Estrut.*, pp. 1–10, 2000.

[7] L. C. Bank, *Composites for Construction: Structural Design with FRP Materials*, John Wiley & Sons, Inc., Hoboken, NJ, USA, 2006. https://doi.org/10.1002/9780470121429.

[8]   American Concrete Institute, *Guide for the Design and Construction of Externally Bonded FRP Systems for Strengthening Concrete Structures*, ACI PRC-440.2-17, 2017.

[9]   R. Salgado et al., "Structural assessment of concrete beams strengthened with CFRP laminate strips by their dynamic response," *Port. J. Struct. Eng.*, vol. 3, pp. 37–46, 2017.

[10] J. Helal et al., "Non-destructive testing of concrete: a review of methods," *EJSE Int.*, vol. 1, pp. 97–105, 2015.

[11] O. S. Salawu, "Detection of structural damage through changes in frequency: a review," *Eng. Struct.*, vol. 19, pp. 718–723, 1997, http://dx.doi.org/10.1016/S0141-0296(96)00149-6.

[12] G. E. S. de Lima, "Avaliação dinâmica do comportamento estrutural de vigas de concreto armado submetidos à degradação da rigidez", M.S. thesis, Univ. Fed. de Viçosa, Viçosa, Brazil, 2017.

[13] M. Ekenel and J. J. Myers, "Durability performance of RC beams strengthened with epoxy injection and CFRP fabrics," *Constr. Build. Mater.*, vol. 21, pp. 1182–1190, 2007, http://dx.doi.org/10.1016/j.conbuildmat.2006.06.020.

[14] H. Nikopour and M. Nehdi, "Shear repair of RC beams using epoxy injection and hybrid external FRP," *Mater. Struct.*, vol. 44, pp. 1865–1877, 2011, http://dx.doi.org/10.1617/s11527-011-9743-8.

[15] S. Griffin, H. Askarinejad, and B. Ferrant, "Evaluation of epoxy injection method for concrete crack repair," *Int. J. Struct. Civ. Eng. Res.*, vol. 6, pp. 177–181, 2017, http://dx.doi.org/10.18178/ijscer.6.3.177-181.

[16] A. W. Leissa and M. S. Qatu, *Vibration of Continuous Systems*, Mc Graw Hill, New York, 2011.

[17] D. E. Branson, "Deflections of reinforced concrete flexural members," *J. Am. Concr. Inst.*, vol. 63, no. 6, pp. 637–667, 1966.

Rev. IBRACON Estrut. Mater., vol. 16, no. 1, e16110, 2023

16/16